



Sensitization of Austenitic Stainless Steels: Current Developments, Trends, and Future Directions

N. Srinivasan¹

Received: 9 October 2020 / Revised: 16 February 2021 / Accepted: 24 February 2021 / Published online: 22 March 2021
© ASM International 2021

Abstract

In this manuscript, the latest developments pertaining to sensitization are discussed. Sensitization leads to intergranular corrosion and intergranular stress corrosion cracking. The advantages and disadvantages of conventional methods to combat sensitization are elaborated. Emerging/newer techniques such as grain boundary engineering, creation of orientation gradients, and high density of twinning to improve resistance to sensitization are also covered. Detection and monitoring of deleterious phase precipitation such as carbides, nitrides, and other intermetallic phases during operation necessitate making use of nondestructive testing (NDT) methods. Possible information that we get from NDT is for material characterization includes the size, shape, and location of a defect. Herein, the significant developments for monitoring and detection of phases concerning sensitization by NDT are discussed. These range from magnetic methods to ultrasonic techniques. The multi-physics approach is essential to fully utilize NDT to ensure/predict the lifetime of the components used in the industry. Further, proper selection of suitable NDT for defect detection can avert accidents, catastrophic failures, and economic losses due to corrosion degradation. For this, the corrosion engineer/corrosionist properly apply the suitable techniques (prevention, monitoring, and assessment) to address the issues of sensitization among the wide choice available.

Keywords Stainless steels · Sensitization · Grain boundary engineering (GBE) · Near-boundary gradient zone (NBGZ) · Electron backscatter diffraction (EBSD) · Magnetic methods · Nondestructive testing (NDT)

Introduction

Corrosion is defined as destruction of material due to chemical reaction between material and its environment. The corrosion is classified into the following: chemical/electrochemical, high and low temperatures, wet corrosion, and dry corrosion. The understanding of exact corrosion mechanism is needed to combat corrosion-related issues. The diverse corrosion mechanism can result in various forms (types) of corrosion. Each form (types) of corrosion tends to have arrangement of anode and cathode at specific locations depending upon the type. These are general or uniform corrosion, intergranular corrosion (IGC), galvanic corrosion, and crevice corrosion, pitting corrosion, erosion corrosion, stress corrosion cracking (SCC), biological

corrosion, filiform corrosion, corrosion fatigue, exfoliation and selective leaching. The simplest form of corrosion is general or uniform corrosion. It implies that degradation starts gradually over the entire surface of the alloy. During uniform corrosion, the materials become thinner until failure occurs. The uniform corrosion rate of austenitic stainless steels can be minimized when passive film (chemically stable, thin, adherent layer having 5 nm thickness that is rich in chromium content) is formed.

A different class of stainless steel exists to meet the demands of various (chemical, petrochemical, household, and building) industries. Hence, the choice of using this alloy requires a complete understanding of metallurgical parameters that dictates formability, mechanical and corrosion properties. These materials, based on their microstructures, are divided into austenitic, ferritic, duplex, martensitic, and precipitation hardening steels. Figure 1 shows that the typical microstructure of austenitic stainless steels consists of three annealing twins. In general, the annealing twins appear in deformed and annealed face-centered cubic (FCC) metallic materials due to growth accidents during the

✉ N. Srinivasan
srinivasan.narayanan@vit.ac.in

¹ Department of Manufacturing Engineering, School of Mechanical Engineering, Vellore Institute of Technology (VIT), Vellore, Tamil Nadu 632014, India

recrystallization of deformed materials. The metallic material that exhibits low stacking fault energy (SFE) tends to form an annealing twin to (1) reduce interfacial energy and (2) to reorient grain boundary (GB) and (3) GB mobility during recrystallization.

Austenitic stainless steels and similar chromium- and nickel-rich alloys exhibit good corrosion resistance, as these are the iron-based alloys with a minimum 10.5 wt% of chromium, which generally do not rust in the unpolluted atmosphere; therefore, it is called as ‘stainless.’ These steels are commonly used for steam generators and structural members due to its inherent high strength and corrosion resistance, against uniform corrosion. The chromium content above 12 wt% is expected to provide a protective passive oxide layer. Passivity is defined as the state of the surface, which exhibits low corrosion rates in the oxidizing environment. However, these materials suffer from localized corrosion due to the breakdown of surface oxide passive film. The intense attack at a discrete site is a typical characteristic of localized corrosion due to breakdown in passivity (Fig. 2a). In general, the

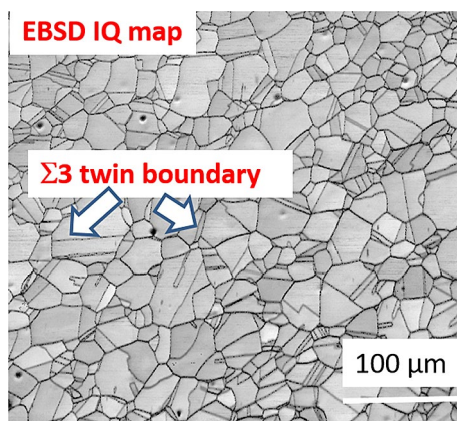
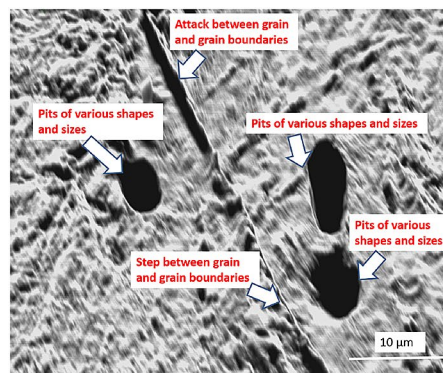
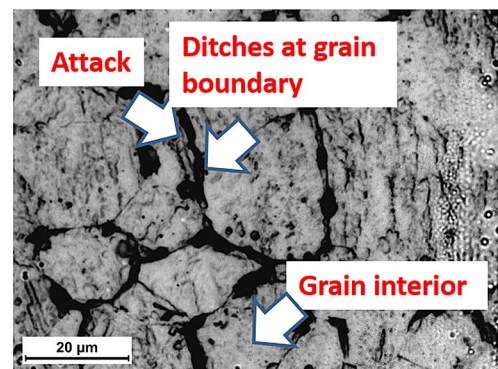


Fig. 1 Electron backscattered diffraction (EBSD) and image quality (IQ) map of as-received specimens of AISI304L austenitic stainless steels

Fig. 2 (a) High-resolution, captured images revealing morphology of pits. (b) Optical microscopic image exhibiting a “dual type of microstructure.”



(a)



(b)

breakdown of passivity refers to the destruction of passive films by mechanical, chemical, or electrical actions.

Sensitization is a process of nucleation, precipitation, and depletion of chromium carbides at/along grain boundaries. Thus, the formation of chromium carbides causes chromium depletion at/along grain boundaries, which leads to pitting corrosion, IGC, and intergranular stress corrosion cracking (IGSCC) of the austenitic stainless steels. IGC is localized corrosion that attacks grain boundary, whilst almost no attack or little attack at the interior of grain. The GB is chemically active and acts as an anode, and the grain acts as a cathode; hence, the IGC-attack happens at/along the GB under corrosive conditions. This is the basis of sensitization (Fig. 3) and leads to premature failure of the engineering components, particularly the boiling water reactors (BWR) in nuclear power plants that usually experience severe

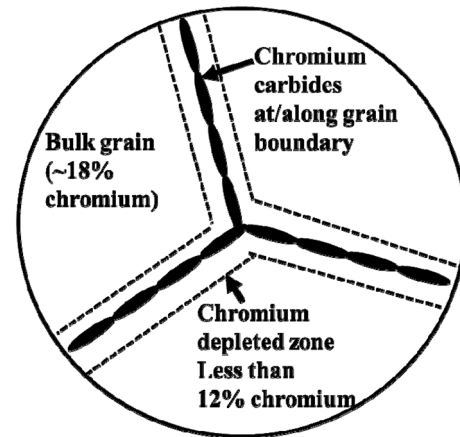


Fig. 3 Schematic diagram of typical sensitized GB having chromium-depleted zone and precipitation of chromium carbides along the grain boundary. Chromium-depleted zones near to adjacent to grain boundaries are termed as sensitized. This leads to IGC [4].

IGSCC of stainless steel in pipeline and core components [1–3].

The factors such as segregation [5], enrichment of precipitates and its depletion of certain alloying element at the GB also increase the severity of IGC. The factors that lead to IGC are uneven thermal exposure and improper heat treatment of metallic materials. Thus, IGC-attack depends on severity of degree of sensitization (DoS) and aggressiveness of the environment.

While classical sensitization is due to the result of thermal exposure around 600–700 °C and the improper welding [6] and heat treatment, on the other hand, the low-temperature sensitization (LTS) usually happens at temperature 300 °C to 500 °C. The present nuclear reactors in India experience this temperature range. During LTS, the preexisting carbides have a chance to grow, and the formation of new carbide precipitation does not occur. The effect of cold rolling on LTS behavior has also been detailed by different researchers [1, 7]. The incidence of IGSCC failures of pipelines in boiling water reactor (BWR) has been reported due to LTS as well as classical sensitization [1, 8].

The DoS explains the extent of chromium depletion at/along grain boundaries due to the nucleation of chromium carbide. The sensitized steels, if allowed to operate, develop crack easily and lead to failures prematurely. Chromium depletion zone is usually characterized by coverage, width, and depth as discussed in this reference [9]. The chromium depletion zone consists of coverage, depth, and width. The depth can be characterized by electrochemical and interferometric profiler techniques. The typical double-loop electrochemical potentiokinetic reactivation (DL-EPR) curves of as-received specimens after sensitization treatment exhibited higher DoS (Fig. 3a).

The fabrication scheme of austenitic stainless steels involves a range of manufacturing activities such as cold/warm working, machining, and a series of surface finishing operations. These activities influence resistance to sensitization due to the generation of plastic strain and residual stress. Generally, cold working of stainless steels generates defects such as dislocations and phase transformation and brings other changes in microstructural features. Further, the cold working of stainless steel changes its grain shape, grain misorientation and GB diffusion rates. The deformation in stainless steel brings the following changes: (1) increase in surface roughness, (2) generation of tensile surface residual stresses, (3) generation of defect density and (4) formation of strain-induced martensite (SIM). These changes accelerate the corrosion-related degradation. The typical DL-EPR curves after small pre-strain (5% and 10% cold-rolled) and sensitized exhibited an improvement in DoS value (Fig. 4b). Hence, cold working influences the DoS (Fig. 4c). Figure 4c shows that slight pre-straining (5% and 10% cold rolling)

increased the resistance to DoS due to diffusion shortcuts as reported in the author's previous studies [10].

Sensitization: the Understandings and Current Developments

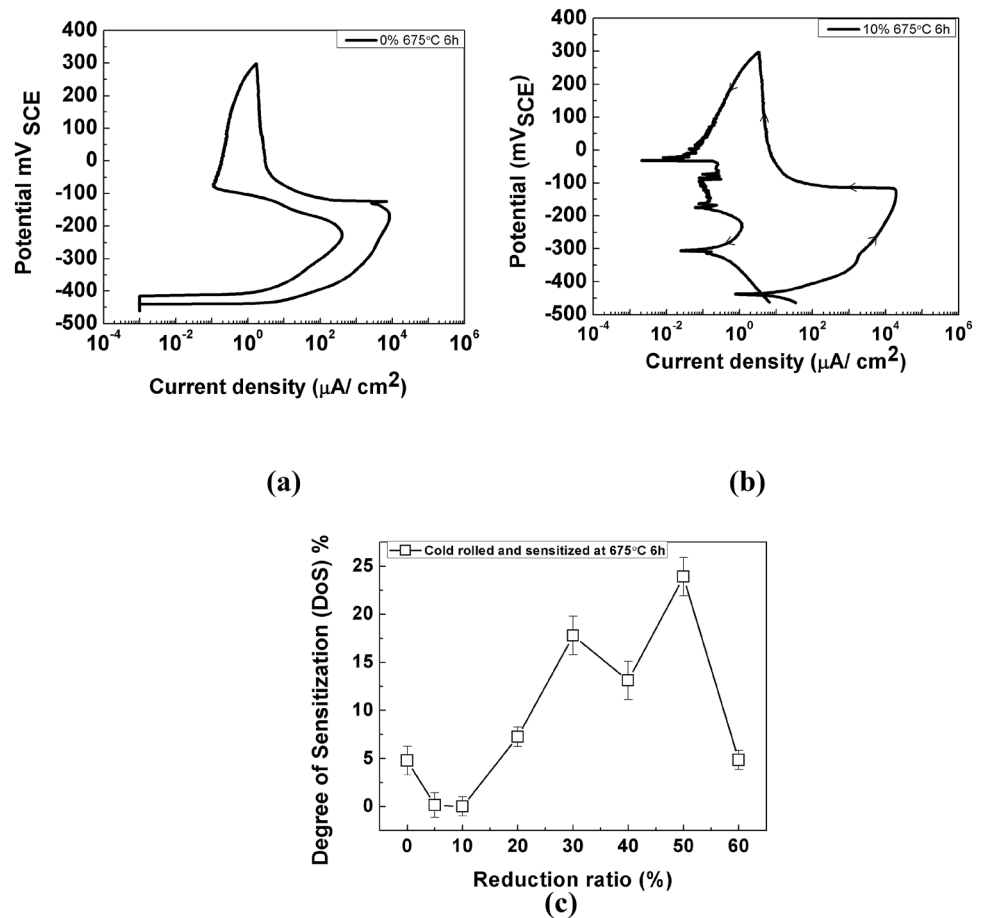
Many researchers have contributed toward the understanding of sensitization of stainless steels that led to IGC and IGSCC-related corrosion issues. Furthermore, many studies have also devoted to studying different factors such as deformation [7, 11–16], grain size [17, 18], grain misorientation [10, 19], GB character [20–22], which affect sensitization kinetics. It is understood that invariably cold working cannot be avoided, and a certain amount of plastic strain is always present in the steels due to manufacturing activities. It is demonstrated by the researchers that the cold and warm working of stainless steels increases the susceptibility to sensitization, and this may lead to IGC and IGSCC. Further, it has been reported that the state of deformation is also shown to affect sensitization [23]. Despite extensive research studies, exactly on the role of deformation and strain-induced martensite (SIM), the researchers have reported conflicting results [24]. The commonly agreed results were till a certain amount of cold-rolling sensitization resistance decrease; beyond certain cold-rolling percentage, desensitization was evident (Fig. 3c).

Further, it has been reported that SIM sensitizes at a temperature of 500 °C [1]. When a specimen of austenitic stainless (austenite phase and non-magnetic) is deformed, it transforms into a martensite phase (magnetic). The DL-EPR test can detect this change of phases by its hump from its curve. The AISI 304 steel specimens that contain a significant amount of martensite exhibited hump in reactivation peak. In general, the martensite is a hard phase, the hardness value of steels increases with increasing amount of martensite.

The detection and quantification of SIM are difficult by X-ray diffraction (XRD); however, it is viable if vibrating sample magnetometer (VSM) and electron backscattered diffraction (EBSD) techniques have been employed [10, 25].

When deformation is increased (medium-higher cold rolling), carbide precipitation occurs at grain matrix than grain boundary. It has been reported that the larger plastic deformation (~ 80–90 % cold rolling reduction) altered microstructure and enhanced resistance to sensitization [26]. In another study, it has been reported that the smaller pre-strain annealing also enhanced resistance to sensitization [10, 27, 28]. Further, it is known that sensitization increases the susceptibility to grain boundary corrosion and hydrogen embrittlement (HE) or hydrogen-induced cracking. The researchers reported that loss of notched tensile strength (NTS) of AISI 304L steels. This loss in NTS has been correlated to

Fig. 4 A typical representation of DL-EPR curves exhibiting (a) lower DoS and (b) higher DoS. (c) the effect of cold working on the DoS of AISI304L stainless steels [10].



hydrogen embrittlement [29]. The sensitized steels generally have higher susceptibility to HE than its as-received/non-sensitized counterpart. The combined effect of tensile pre-strain and sensitization on susceptibility to HE was also explored in another study [30]. In this work, it is reported that preexisting SIM particles can increase the chances for HE susceptibility of sensitized 304. The effect of grain size on sensitization has also been studied by the researchers since long time. The contradiction does exist on the effect of grain size on sensitization [17, 23, 31–33]. The 304L steels with grain sizes below $10 \mu\text{m}$ increased DoS [17]. On the contrary, it has been reported that higher average grain size ($> 89 \mu\text{m}$) developed few chromium carbide precipitations. This has increased resistance to sensitization [32]. The DoS decreases with increasing grain size [32, 33]. It has been reported that, in larger grain size, the chances of carbide precipitation are delayed [32]. However, it is suggested that arriving at optimum grain size without compromising the mechanical properties can be the best strategy for increasing the resistance against IGC-attack. Thus, the role of grain size on sensitization is controversial and remains challenging till now [34]. Further, it has been reported that EBSD-based image quality (IQ) value has also been used to detect DoS [35]. The IQ (diffraction contrast) value relates

to the crystallinity. The lower value of IQ has shown to be decreased resistance to sensitization. This observation was confirmed with DL-EPR curves. The difference in value of IQ at phases has attributed to precipitation of carbides.

The new approach has been emerged to control sensitization, though crystallographically has also been discussed [22, 36]. On the one hand, Fuji et al. [22] have shown that the absence of IGC attack at low-angle GBs (misorientation between 5° and 10°) and IGC attack observed low-angle GBs of misorientation between 10° and 15° [22]. On the other hand, manipulating a microstructure with regions of heavily twinned microstructure improved the resistance to sensitization [36].

In addition, by populating (area fraction of 3 recrystallization twin) high density of twinned microstructure in 304 steels, increased resistance to IGC has been shown [37]. In another study of sensitization of Al–Mg alloy series, it was reported that the low-angle boundaries (8.7°) arrested the development of IGC. This immunity was attributed to the presence of discrete β phase [38]. Excessive plastic deformation (abusive or rough machining) of austenitic stainless steels leads to generation of SIM, decrease in ductility, misfit between parent and product phase [39]. The vertical milling practice of stainless steels distorted the grains as

observed by EBSD measurements (Fig. 4) of stainless steel specimens. It has been shown that the effect of machining-induced subsurface was detailed in this study [40]. Further, its machining (milling) generates subsurface (Fig. 4), thermal energy, and residual stresses also that affect the kinetics of sensitization [41]. The exhaustive review about the role of machining/working on SCC has been detailed in this reference [31, 42–44].

Normal practice is that the typical corrosionist looks at the development of the SCC-related issues and the machinist looks only at generation of residual stresses. The influence of machining (varying degrees of machining) on classical sensitization and LTS has been less explored; however, the effect of machining-related corrosion issues leads to the development of surface cracking, IGSCC has been extensively explored by the researchers [40, 43, 45], and particularly different surface working/finishing operations such as grinding, milling, turning and buffing have also been shown to affect the performance of stainless steels due to SCC (Fig. 5).

Mitigation Strategies Adopted

The mitigation approach to control sensitization has been investigated by researchers since 1920. These include traditional approach (alloy chemistry [46, 47], carbide formers, solution annealing, solute atoms) to emerging techniques. These are detailed below.

Chemistry

Limiting carbon content to concentrations below 0.03% (extra low concentrations) usually reduces the chance for the formation of chromium precipitation and its depletion. Further, increasing nitrogen, manganese, chromium, and molybdenum enhances the resistance to sensitization. Usually, carbon and chromium are the dominant compositional variables that increase susceptibility to sensitization. The role of copper in austenitic stainless steel is to stabilize austenite and increase uniform corrosion resistance. This addition of copper entails cost-saving as it is added as an alternative to nickel, as nickel is expensive [48].

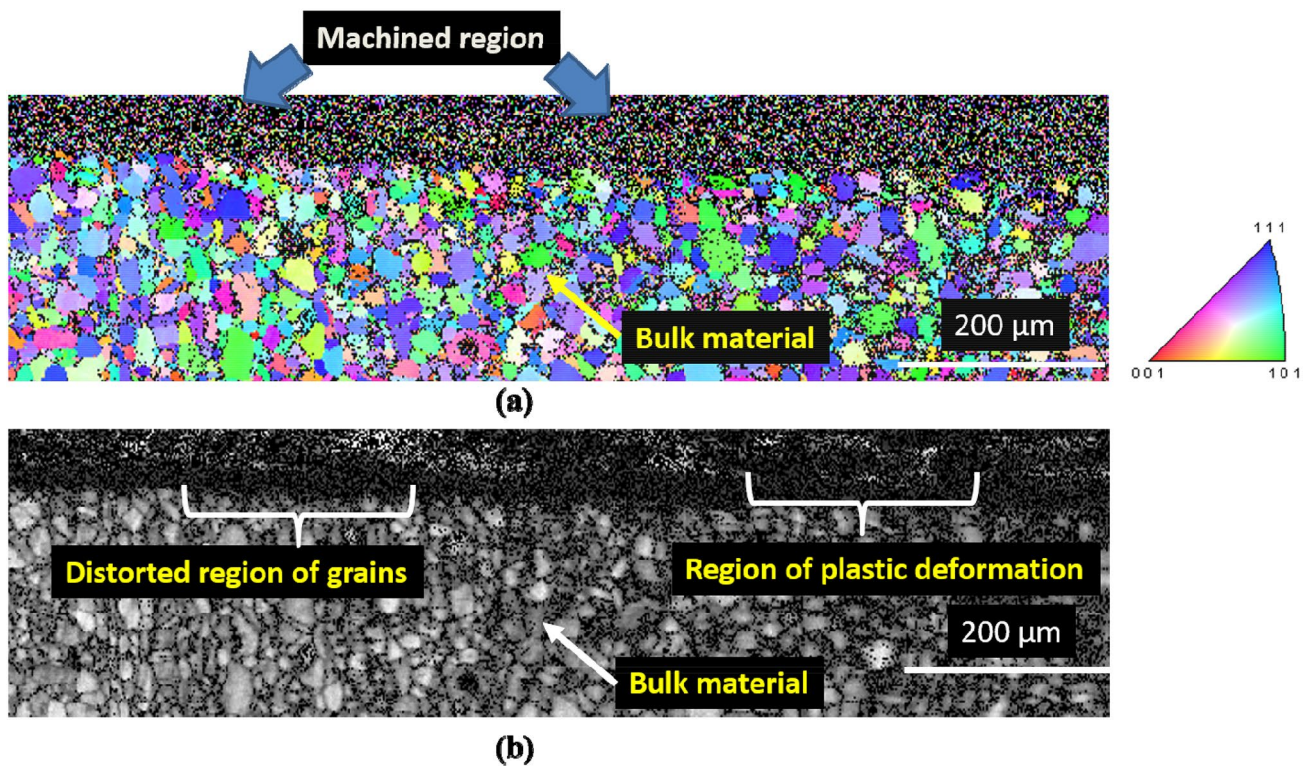


Fig. 5 The milled (machining) region of AISI304L stainless steels as observed (a) EBSD inverse pole figure (IPF), (b) IQ map

Carbide Former

To mitigate sensitization of stainless steels, their chemical composition is altered with austenite stabilizers such as titanium (Ti), niobium (Nb), columbium, and mixtures of columbium–titanium mixtures. These chemical elements are regarded as austenite stabilizers. Hence, Nb and Ti elements are added to stainless steels to impart resistance against sensitization. Farahat et al. have shown that AISI 316 steel with 0.412% Nb and 1.1% Ti has exhibited no sensitization after 675°C for 1-h heat treatment [49]. This resistance has been attributed due to the absence of carbides agglomerate at near GB.

Solution Annealing

Solution annealing (SA) is a heat treatment process that is usually performed before its actual use in industries. SA is an important step in sensitization control [50]. This technique may increase in grain size and introduce large thermal stresses due to rapid quenching. This technique is almost impracticable for large, complex, and bulk components used in nuclear and chemical industries. Further, this treatment increases grain size [49, 51–53]. IGC in stabilized grades of austenitic stainless steels has been reported to be chromium segregation near/at grain boundary [52]. The precipitation of $M_{23}C_6$ is possible at the temperature range of 400 °C to 950 °C. The SA temperature for the conventional stainless steels such as AISI 201, 202, 302, 302, 303, 304, 305, and 308 is generally in the temperature range of 1020°C to 1120°C. The objective of SA is to dissolve preexisting deleterious phases present in the stainless steels. It is also reported that these deleterious phases have also been formed during thermomechanical processing (TMP). The final stage in TMP always involves SA. Although this method can be considered as an effective mitigation strategy, often it has the risk of grain growth. The criticality of using this strategy is limited to choosing the optimum SA temperature. Before deciding, besides, the geometry of stainless steel components should be considered. It needs to be considered that laser surface technology is emerging as a technological step for mitigating sensitization [50, 54]. These emerging techniques are discussed separately in this manuscript. These are: (1) addition of oversize solute atoms [55], (2) altering grain boundary nature and connectivity [20, 21, 34], (3) populating high-density twinning [36, 37], and (4) through providing a near-boundary gradient zone (NBGZ) [10, 28].

Solute Atoms

It has been shown that the addition of cerium (Ce) to steels improved the resistance against sensitization [55, 56].

Grain Boundary Engineering

Grain boundary engineering (GBE) is a well-established, effective, and inexpensive method of improving the properties of polycrystalline materials that use thermomechanical processing (TMP) [57, 58]. TMP enhances the property (strength, creep resistance, SCC, hot corrosion, and oxidation, particularly pronounced more in austenitic stainless steels and Ni-base alloys) by altering grain boundary nature and connectivity to increase the resistance against corrosion-related issues [59]. This has been well documented since the 1980s by the researchers through several independent studies for austenitic stainless steels and other alloys. There are two approaches for the implementation of TMP, and they have been widely explored by the researchers [60–62]. These are (Fig. 6) (i) strain annealing and (ii) strain recrystallization. Strain annealing is a single-step process that imparts a small amount of pre-strain on the specimen with prolonged heat treatment. The strain recrystallization is an iterative, multi-pass rolling and heat treatment process for effective grain boundary control. In this approach, a moderate degree of plastic strain is imparted on the specimen followed by short heat treatment. With this approach, the microstructure is manipulated with a high fraction of special boundary (special boundaries) and connectivity of random boundary network.

The grain boundary-engineered materials exhibit higher population of coincident site lattice (CSL). The CSL model describes grain boundary character distribution (GBCD) by classifying low CSL, high CSL, and random grain boundaries. Thus, the main objective of GBE is to manipulate microstructure that discourages the initiation and propagation of intergranular degradation by disconnecting random grain boundary network and then introducing low-sigma CSL boundaries. In precise, the introduction of small pre-strain and high-temperature annealing is a way to increase special boundary concentrations, and this has been considered as an effective way to enhance resistance to sensitization [27]. In contrast, another approach of extremely randomizing grain boundary network improved the resistance to sensitization [26]. They have shown that introduction of large plastic deformation (approximately 85% of

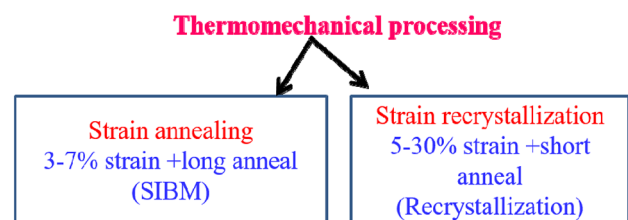


Fig. 6 The two approaches of thermomechanical processing

cold rolling) has produced extremely randomized grain boundary [26]. The thermomechanical processing typically imposes small pre-strain [27, 63], and single-step annealing is generally employed to obtain desired corrosion properties. This processing modifies microstructural features (grain size, residual strain, GBCD, and GB topology). It is further reported that the grain boundary-engineered microstructure [34, 59] and GB network topology [20] of type 304L stainless steels exhibited resistance against sensitization.

In recent times, grain boundary junction engineering (GBJE) or triple junction engineering [64] is getting attention among researchers for enhancing the structure–property relationship for low SFE FCC materials. It is a branch of grain boundary engineering (GBE) that deals with triple junction (TJ) (Fig. 6) and its connectivity [65]. TJ consists of CSL and random boundaries (Fig. 7). The formation of TJ happens when grains (three) meet respecting crystallographic rules, which are characterized according to Fortier et al. [27] and classified into 4 types, namely (1) three special boundaries (S–S–S or 3-CSL or J_3), (2) two special boundaries and one random boundary (S–S–R or 2-CSL), (3) one special and two random boundaries (S–R–R or 1-CSL), and (4) three random grain boundaries (R–R–R). To understand continuous percolative paths and to determine triple junctions that offer resistant GBE microstructure, based on types of triple junction originally proposed by Fortier et al. [27], Kumar et al. [28] suggested a resistant triple-junction parameter, i.e., $f_{2\text{csl}}/(1-f_{3\text{csl}})$, where $f_{2\text{csl}}$ is the frequency of two CSL and one random boundary, and $f_{3\text{csl}}$ is the frequency of three CSL boundaries. The analysis of grain boundary connectivity using orientation imaging microscopy (OIM) reveals information about clusters of random boundaries [66] and its length for the entire grain boundary network. In general, the improved resistance to sensitization (or localized interfacial degradation or grain

boundary-sensitive material properties) is observed when there is connectivity of special boundaries (CSL boundaries) and disconnectivity of random grain boundaries.

Orientation Gradients

In general, plastic deformation of metallic materials develops grain-specific misorientation, called as near-boundary gradient zone (NBGZ) that signifies the presence of dislocation. The dislocation theory and crystal plasticity are also used to characterize NBGZ. The grain interior and its interaction between near neighbors are shown to affect material properties such as mechanical and corrosion properties. It has been shown that previously by the present author that the larger the region of NBGZ, the better the immunity toward corrosion properties [10, 28]. The graph (normalized distance vs misorientation) illustrates calculation of such orientation gradients (NBGZ) for a typical grain (Fig. 8a). The grain center is identified, and line vector is drawn. The misorientation spread and distance are calculated. More information is available in this reference [10, 67, 68]. The deformed microstructure with regions of NBGZ (10% cold-rolled specimen) (Fig. 8b) provided resistance to sensitization [10, 68].

Other Techniques (SMAT, LSM)

The coherent and high-energy beams (lasers, electron beams) have been used for surface property enhancement for a long time. These sources are used to melt phase transformation [69] of surface regions. In laser surface melting (LSM), a thin layer is melted by laser sources (Nd:YAG, CO₂ and Ruby). During melting, carbides and impurity are reduced. The other emerging techniques make use of modifying surface microstructure without changing bulk properties. Surface engineering is a method to alter the microstructure and composition of the near-surface region for enhancing certain properties of materials such as corrosion and wear resistance. In precise, surface engineering deals both microstructural and compositional modifications. LSM and surface mechanical attrition treatment (SMAT) deal with microstructural/surface modifications. Surface engineering deals with changing the properties of near surface to enhance the performance of engineering components over time [70]. It is also reported that LSM addresses the issues of cavitation erosion [71], IGC [72, 73], and pitting corrosion [74]. The influencing process parameters are reported to be pulse width, linear speed, gas pressure, and pulse repetition rate [72]. Further, to avoid the breakdown of components, failure of equipment, the nucleation and growth of pits, and arrest of cracks, the sensitized microstructure can be treated with the LSM technique. SMAT is a method to the synthesis of surface nanolayer by employing shots (milling balls) to

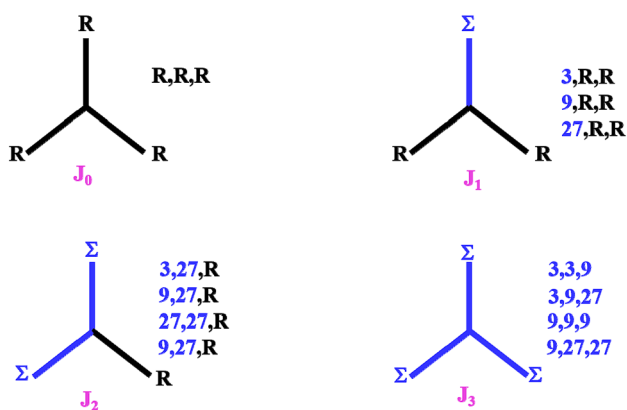


Fig. 7 Triple junction (TJ) (J_0 , J_1 , J_2 , J_3) types with a combination of boundary types (random grain boundary and CSL boundary). The J_0 represents a junction having three grains connected with random (R, R, R) boundaries.

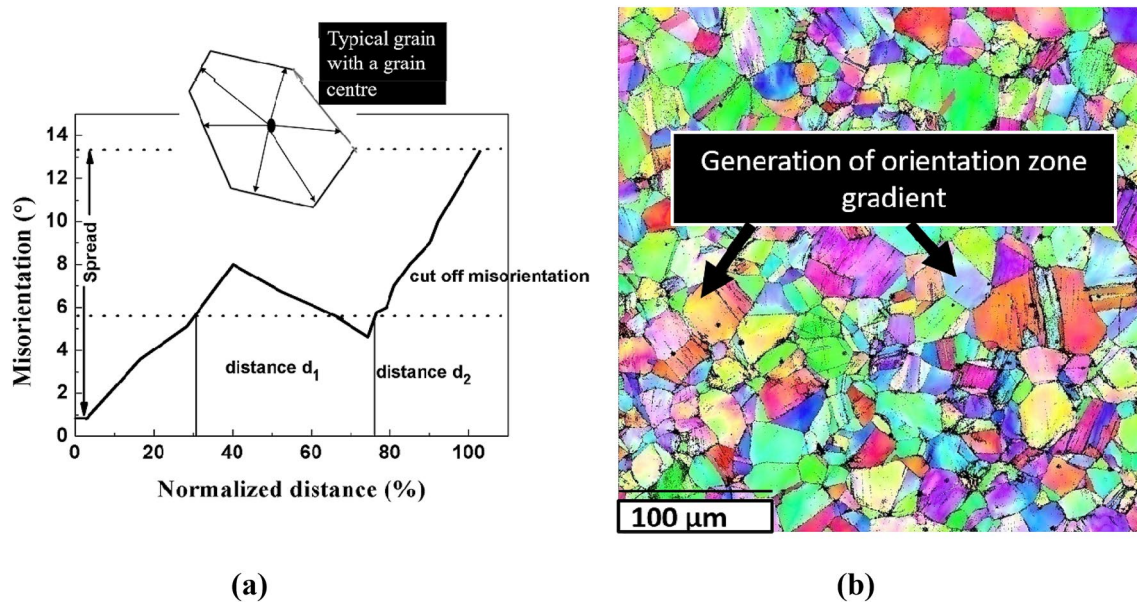


Fig. 8 (a) Quantification and (b) microstructure with regions of NBGZ.

enhance mechanical and corrosion properties. It has been reported that SMAT enhanced the resistance against sensitization for AISI 316 steels. However, this method is also without its drawbacks. The major disadvantage is the issue of surface roughness and generation of surface cracks due to continuous impacts. Compared with other surfacing methods, LSM is considered feasible for mitigating sensitization and arrest sealing cracks. The LSM process is a rapid solidification process. In another study, it has been reported that LSM improved pitting resistance [75]. Besides, it is reported that LSM increases the stability of the austenite phase and yield strength [76]. Mudali's group has been the pioneer in this field addressing sensitization through LSM technology. In this work, the IGC susceptibility of 304 stainless steel was evaluated, and a higher population of twin boundaries arrested the IGC attack [37]. The twin boundary is a low energy boundary that arrests the carbide precipitation at the grain boundary.

LSM is also without the disadvantages. LSM is likely to result in duplex microstructure in austenitic stainless steels and ensures the phase balance for duplex stainless steels. This method is in situ to selectively remove the sensitized microstructure at critical locations. The change in microstructural features is usually studied by typical metallographic technique, hardness, and mechanical test. These mentioned techniques are destructive, and specimens may not be used again for any use. Although it is very effective to detect sensitization, it is difficult to detect the components or structures which are already in use (production or service). Hence, the need for testing the components or structures

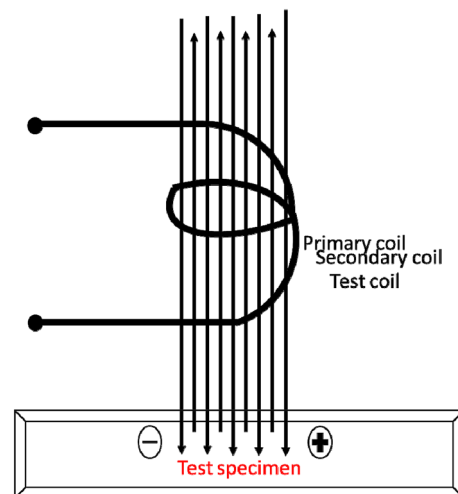


Fig. 9 The schematic of working principle eddy current testing device

demands the methods which are of a nondestructive type and in situ [77].

Evaluation of Sensitization: Emerging Methods

Over the years, the sensitization of austenitic stainless steels has been investigated by different techniques/methods. These are Huey and Strauss tests, single-loop [78, 79] and double-loop EPR [80, 81], local electrochemical impedance

spectroscopy (LEIS), electrochemical noise technique [82], eddy current testing (EDT) (Fig. 9).

In order to assess the components of stainless steels for sensitization after a fabrication process or during in-service, the different techniques/methods have been used. These are varied between typical etch test and electrochemical test to sophisticated techniques such as NDT- and magnetic-based methods [83]. The traditional methods include oxalic acid etch test and electrochemical technique such as electropotentiokinetic reactivation (EPR) tests. These methods have been used widely for laboratory-based assessment. For inspection of stainless steel components, during in-service, the NDT-based acoustic [84], ultrasonic measurements thermoelectric power (TEP) [85], and magnetic-based measurements such as eddy current techniques, magnetic force microscope (MSM) [86], and atomic force microscopies [87] have been used.

Strauss, Huey, and Streicher tests require a lot of specimens and cannot be performed in situ, and sensitivity for detecting lower DoS is an issue. There is a need for quantifying the effect of fine precipitation and depletion; EPR tests have been developed in 2.5M H₂SO₄ test solutions (Cihal 1969); further, Clarke et al. proposed single-loop EPR in test solutions of 0.5M H₂SO₄ + 0.01M KSCN. These EPR techniques need a very fine surface finish; hence, this requires time for the preparation of specimens. Akashi et al. developed DL-EPR test methods. This method overcomes inclusion content and quality of surface finish. To overcome limitations of chemical tests, an electrochemical technique called electrochemical potentiokinetic reactivation (EPR) method has been developed [78, 88–91]. The early detection of sensitization and other IGC-related corrosion degradation is considered very important for the safe and efficient operation of plants.

The NDT methods have been gaining acceptance, for maintaining the structural integrity and health monitoring of engineering components and making situation-based maintenance judgments (decisions) in any power plants/factory. Further, monitoring and assessing the impact of corrosion degradation help to achieve early detection of defects in specimens from the fabrication stage to the operation/service stage. Furthermore, the NDT is also emerging as an alternative method to find out the root cause of any failures and to take appropriate preventive actions in any plants/industry, particularly for pressurized water reactor (PWR) and boiling water reactor (BWR). In this direction, the conventional acoustic emission (AE) [84, 92], linear ultrasound (LU) [93], nonlinear ultrasound (NLU) [94, 95], and magnetic-based techniques such as EDT [96, 97] (Fig. 8), induction infrared thermography [98, 99], and magnetic Barkhausen noise (MBN) have been used to study the development of sensitization-lead IGC issues [84, 100–103]. The AE is a wave that travels at the speed of sound, and the LU is an

acoustic wave with higher frequency (humans can't hear); on the other hand, humans can hear infrasonic wave and subsonic wave, as both infrasonic and subsonic waves travel less than the speed of sound. The AE is based on the release of transient elastic wave (energy) within the material. When pits propagate, the recorded AE signals become apparent [100]. The detected signal of AE consists of event number, amplitude, rise time, count number, duration, and nonlinearity parameters (β). These parameters can be related to the presence of precipitates, chromium depletion zone, and dislocations [95]. The higher value of measured β indicates an absence of sensitization. The ultrasound is generally non-destructive and non-ionizing acoustic waves, that propagate through elastic media. Longitudinal waves are the most common form of ultrasound propagation. As there is no radiation exposure for using ultrasonics, this increases the safety of a technician/operator. The ultrasound is a sound wave with frequencies above 20KHz.

The nonlinear ultrasound (NLU) has also been used to characterize the materials' damage using the information from attenuation, the amplitude of peaks, wave velocity, attenuation, and spectral peak. To overcome the problems associated with LU in assessing the IGC, the NLU (harmonics generation) has been used by the researchers. The linear ultrasonic-based NDT methods have been used since 1970s in the use for the medical industry. Of late, this technique is well suited to detect the location of defects, flaws, and voids. The NDT methods such as ultrasonic and eddy current testing have limitations or have inaccurate in detecting the initial stage of IGC and IGSCC; the author has used the laser scattering studies [104]. The conventional ultrasonic parameters are usually sensitive to bulk properties; hence, any changes in bulk are detected. Hence, it is not suitable for detecting the initiation of localized corrosion. The alternative to this is the use of nonlinear ultrasonics by generating harmonics [105] and laser-based scattering techniques [104] and wave mixing techniques [105]. In another study, NLU Rayleigh waves have been used to assess sensitization [92]. Rayleigh waves (Fig. 10) are nonlinear surface acoustic undulating waves that propagate along the surface of solids. Since the IGC attack is usually at the micro-level generally, the low depth penetration of LU for detection of macro-level cracks may not bring out the actual state; hence, different operating parameters as mentioned previously help to provide better information about IGC-attack. For detecting IGC for aircraft



Fig. 10 The Rayleigh waves

aluminum alloys, X-ray tomography was used [106]. However, the detected nonlinearity parameter β is from material damage or due to configurations of equipment such as transducers and amplifiers. To overcome this, the alternative method is to use the wave mixing technique (both co-linear and non-co-linear). Mudali et al. [104] came up with a laser scattering technique, and Jingpin et al. [105] came up with a wave mixing technique. The researchers have established the correlation of laser scattering parameters with IGC attack.

Rayleigh waves are generally used to characterize mechanical and structural properties. Rayleigh waves are surface acoustic waves that propagate the surface of solids. In this method, the nonlinearity parameter β has been used to confirm the presence of $M_{23}C_6$ carbides. The predictions of structural changes in materials at the early stages by the nondestructive way (ultrasonic wave propagation) are relevant. It is used to characterize the initiation and growth of cracks due to IGSCC as its harmonic waves contain information about the change in microstructural features (precipitates, dislocations, voids, radiation damage, fatigue damage, and residual stresses). The acoustic nonlinearity parameter β is particularly useful for field applications. The theoretical background and approach to this technique are detailed in these references [92, 107]. The experimental technique and arrangement of air-coupled devices, transducers, and amplifiers are placed as shown in figure. The researchers demonstrated that acoustic nonlinearity parameter β has been sensitive to microstructural changes due to various processing/operating conditions such as sensitization-lead IGC and IGSCC. Further, the parameter β was well correlated with EPR measurements. The precipitation of sigma phase is due to thermal aging in duplex stainless steels [107] and chromium carbide due to sensitization in austenitic stainless steels [92]. The increase in β indicates generally an absence of deleterious precipitates such as sigma phase and chromium carbides. The usage of transducers based on their frequency can yield information about a low degree of sensitization; hence, it is usually recommended that proper selection and usage are important. The increase in ultrasonic attenuation information can provide a good picture of sensitization developments. Theoretical understanding of precipitation that leads to sensitization is possible. The researchers have reported that by generating harmonics (nonlinear ultrasonics) the early deterioration of IGC has been studied extensively. However, this also the without limitations, to overcome wave mixing technique is proposed. The electromagnetic acoustic transducer is a non-contact type (does not require contact or couplant); an ultrasonic NDT instrument measures ultrasonic velocity and attenuation. It is reported that ultrasonic velocity information did not reveal about DoS and shear velocity, and attenuation revealed DoS in AA5XXX aluminum alloy [108]. The same was observed for 304 stainless steel [109]. Thus, the early detection leads

to a longer lifetime of components and structural failures as reported. In practice, during in-service of components the failure due to sensitization is usually several times higher than the carbide saturation limit. Thereby to address the advanced sensitization stage, NDT-related techniques such as EMAT, UT are useful and justified from a purely practical point of view [109]. Conventional NDT techniques can overcome the problems associated with EPR methods. ECT is considered as a suitable alternative to be able to monitor in-service sensitization as it can detect changes in electrical conductivity and permeability [96]. In ECT, when an alternating current is passed to the specimen, the magnetic field is developed proportionately to the applied current. If other conducting specimens are into this magnetic field, then current will be induced to these specimens. The appreciable amplitude change in eddy current signal indicates $M_{23}C_6$ types of carbide depletion.

If any structural variations present in the specimen affect/decrease the eddy current, the ECT can be used for the thickness of materials and coatings, detection of cracks, and conductivity measurements to identify materials. Furthermore, the applicability of ECT has extensive [96, 110]. In another study, ECT has been used to find the martensite phase present in stainless steel [110]. These authors also indicated that with the help of reference specimens, it is possible to substantiate the result of ECT measurements. ECT works well only on the IGC-attacked areas; hence, it is very important to select suitable techniques based on the specimens testing requirement [105]. Thus to explore other avenues for measurement of sensitization, the researchers explored the feasibility of magnetic methods. The superconducting quantum interference device (SQUID) magnetometer-based VSM has been used for the measurement of sensitization by generating magnetic hysteresis curve (also known as M-H curve). The SQUID consists of two superconductors separated by an insulating layer, forming a Josephson junction. When a very thin insulating layer is placed between two superconductors, then a continuous super-electric current is generated without the application of voltage. This is known as Josephson effect. It is based on tunneling superconducting electrons. The SQUID measures the magnetic fields, whereas VSM measures the magnetization of a specimens. The saturation magnetization and coercivity measurement from hysteresis loop give information about the volume fraction of α phase. The magnetic properties are sensitive to the structure of metallic materials, as it measures subtle magnetic fields. The NDT-based magnetic measurement techniques have been gaining attention for the detection of defects such as initiation and presence of subsurface cracks. The chromium depletion at grain boundary has also been measured by magnetic force microscopy [34]. In VSM, the specimen is usually placed in a uniform magnetic field H , and magnetization M is induced in a sample. In this, specimen is

placed between two electromagnetic pieces and it is made to oscillate by vibrational unit. In another study, magnetic hysteresis loops of stainless steels have been assessed by VSM [35]. The saturation magnetization (M_s) and coercivity (H_c) measurements have been used to evaluate the magnetic properties. M_s is defined as maximum magnetism state the materials can experience when magnetic field (H) is applied. At larger values of H , the magnetization M becomes constant at its saturation value M_s . Paramagnetic signal is from matrix, and ferromagnetic signal is from localized Cr-depleted regions. The authors concluded that increased ferromagnetic signal could be from local Cr-depleted regions. However, the authors concluded that sophisticated portable magnetic characterization techniques will replace before this can serve as an alternative to assess sensitization in stainless steels. Further, to use as a standalone techniques in industries, it needs to be checked and calibrated every time before using with the reference specimens of known sensitization values. The magnetization curves usually have been measured by a VSM. The chromium depletion at grain boundary has also been measured by MFM [83]. In VSM, the specimen is usually placed in a uniform magnetic field H , and magnetization M is induced in a sample. In this, a specimen is placed between two electromagnetic pieces, and it is made to oscillate by the vibrational unit. This is helpful for both new and aged nuclear power plants.

Closing Remarks

In this manuscript, it is clearly shown that significant developments have taken place in the area of sensitization. Furthermore, this chapter has provided up-to-date information about sensitization; this includes newer mitigation strategies and assessment schemes adopted by the academicians and researchers. The creation of NBGZ and the high density of twinned structures have shown to improved resistance to sensitization. For instance, during the manufacturing of austenitic stainless steels, selection of proper fabrication schedule and/or thermomechanical processing creates NBGZ; then, the problem of sensitization can be minimized. Further, the SA of final components also mitigates the issue of sensitization.

The alternate methods, mainly conventional and magnetic-based NDT methods, were presented in this chapter for quick assessment of sensitization, and these techniques have more application advantages, particularly inspecting in-service equipment. This has been considered to be an effective tool for quality control and fabrication of products. This can serve as a piece of additional information that guides the corrosion engineer/corrosionist to make an appropriate decision, along with the traditional techniques. Because the output of NDT (results) can be subjective. A

suitable interpretation by the field specialist to arrive at the possible solution is needed.

For instance, the NDT-based nonlinear ultrasonic Rayleigh techniques are well suited for on-site application to assess the damage. Most of the time, as it requires testing the specimen on one side during the operation in the plants/industries. Hence, the proper selection of techniques/tools for assessing the damage needs vast knowledge about the latest technology that is available in the market. Furthermore, the magnetic-based NDT methods such as ECT and magnetic Barkhausen noise (MBN) can detect the changes in microstructural features. The output of ECT is impedance and harmonics. The changes in these parameters can be related to changes in microstructural features. Hence, the proper selection of method for the assessment of sensitization is at the discretion of corrosionist, in-service plant field operators. All these methods can be applied independently, and for validation of results, usage of either reference specimens or conventional methods is apparent.

The stringent guidelines demand the use of new, advanced, and innovative technologies for quick assessment of locating defects and for online monitoring of structural damages and initiation of cracks. Thus, the effective corrosion monitoring strategies if implemented are in-place; then, the unexpected and sudden closure of plants can be avoided. The regulation authorities of engineering industries in general and particularly the nuclear industry ensure safety in all respects. In the nuclear energy field, minor defect in components leads to violation of safety codes/procedure and standards. This violation is usually looked at seriously. Usually, the plants and any typical engineering industry particularly require constant inspection and regular maintenance for ensuring safety and improving efficiency. To address this, ISI techniques/methods are employed to ensure structural integrity and safety periodically during maintenance outages.

In this direction, the regulatory authorities of all nuclear power-producing countries across the globe constitute an in-service inspection (ISI) program that guarantees early detection and evaluation of defects that lead to failure of components. The ISI is a periodic nondestructive examination of the nuclear power plant to provide the current state of the plants. The scope of ISI includes active maintenance, surveillance, as this ensures the adequate safety of all components and parts of the plants within the operational limits and conditions. Further, the ISI program ensures preventive failure analysis, maximizes safety, prevent production losses, and enhances the performance of nuclear power plants. The ISI utilizes the NDT as a key tool for its successful implementation; for this, the proper understanding of available NDT/other methods, educated guess, calculated risk, and scientific approach is needed. When the corrosionist anticipates failure of components, for taking appropriate action

and removing the hazard, the time frame is usually adequate. Furthermore, the early, proactive detection of corrosion cracks and their related issues result in savings and record in increased revenue. During ISI, typically three different NDT methods are applied. These are visual, surface, and volumetric examinations. The issue of IGSCC in stainless steels has been encountered in BWR recirculation pipelines. The same has been experienced in dissimilar metal welds in PWR and BWR plants. Furthermore, NDT has been used to detect IGC and IGSCC in a dry cask storage system (DCSS). The dry cask is a metallic (steel) cylindrical container to store hazardous and radioactive nuclear waste materials such as spent nuclear fuel. The DCSS provides leak-tight proof containers that provide radiation shielding and preventing further nuclear fission. Several NDT methods have been used for monitoring and surveillance of DCSS for the detection of cracks and estimating its size. Hence, the application of NDT methods is promising and encouraging; however, the accuracy and reliability depend on the expertise of the NDT operator. The abundant experience and suitable interpretation of NDT result in save components to make informed decisions

References

- Kain V, Chandra K, Adhe KN, De PK (2004) Effect of cold work on low-temperature sensitization behaviour of austenitic stainless steels. *J. Nucl. Mater.* 334:115–132
- Lozano-Perez S, Yamada T, Terachi T, Schröder M, English CA, Smith GDW, Grovenor CRM, Eyre BL (2009) Multi-scale characterization of stress corrosion cracking of cold-worked stainless steels and the influence of Cr content. *Acta. Mater.* 57:5361–5381
- Gordon BM (2013) Corrosion and corrosion control in light water reactors. *Jom.* 65:1043–1056. <https://doi.org/10.1007/s11837-013-0658-4>
- Engelberg DL (2010) 2.06—intergranular corrosion. *Shreir's Corros.* 2:810–827
- Wang J, Shi W, Xiang S, Ballinger RG (2021) Study of the corrosion behaviour of sensitized 904L austenitic stainless steel in Cl⁻ solution. *Corros. Sci.* 181:109234. <https://doi.org/10.1016/j.corsci.2020.109234>
- Kumar S, Shahi AS, Sharma V, Malhotra D (2021) Effect of welding heat input and post-weld thermal aging on the sensitization and pitting corrosion behavior of AISI 304L stainless steel butt welds. *J Mater Eng Perform.* <https://doi.org/10.1007/s11665-021-05454-4>
- Singh R, Chowdhury SG, Das G, Singh PK, Chattoraj I (2012) Low temperature sensitization on the orthogonal surfaces of prior deformed AISI 304LN and aged at 673 K to 873 K (400 °C to 600 °C). *Metall. Mater. Trans. A.* 43:986–1003
- Kain V (2011) Stress corrosion cracking (SCC) in stainless steels. In: Raja VS, Shoji T (eds) *Stress Corrosion Cracking Theory and Practice*, 1st edn. Woodhead Publishing Limited, Cambridge, pp 199–244
- Kain V, Prasad RC, De PK (2002) Testing sensitization and predicting susceptibility to intergranular corrosion and intergranular stress corrosion cracking in austenitic stainless steels. *Corrosion* 58:15–37
- Srinivasan N, Kain V, Birbilis N, Mani Krishna KV, Shekhawat S, Samajdar I (2015) Near boundary gradient zone and sensitization control in austenitic stainless steel. *Corros. Sci.* 100:544–555
- Ramírez LM, Almanza E, Murr LE (2004) Effect of uniaxial deformation to 50% on the sensitization process in 316 stainless steel. *Mater. Charact.* 53:79–82
- Alvarez C, Almanza E, Murr L (2005) Evaluation of the sensitization process in 304 stainless steel strained 50% by cold-rolling. *J. Mater. Sci.* 40:2965–2969
- Singh R (2008) Influence of cold rolling on sensitization and intergranular stress corrosion cracking of AISI 304 aged at 500 °C. *J. Mater. Process. Technol.* 206:286–293
- Jinlong LV, Hongyun L (2012) Influence of tensile pre-strain and sensitization on passive films in AISI 304 austenitic stainless steel. *Mater. Chem. Phys.* 135:973–978
- Solomon N, Solomon I (2017) Effect of deformation-induced phase transformation on AISI 316 stainless steel corrosion resistance. *Eng. Fail. Anal.* 79:865–875. <https://doi.org/10.1016/j.engfailanal.2017.05.031>
- Zhang X, Tang J, Liu H, Gong J (2019) Effects of pre-strain on sensitization and intergranular corrosion for 304 stainless steel. *Eng. Fail. Anal.* 106:104179. <https://doi.org/10.1016/j.engfailanal.2019.104179>
- Singh R, Chowdhury SG, Ravi Kumar B, Das SK, De PK, Chattoraj I (2007) The importance of grain size relative to grain boundary character on the sensitization of metastable austenitic stainless steel. *Scr. Mater.* 57:185–188. <https://doi.org/10.1016/j.scriptamat.2007.04.017>
- Kolli S, Javaheri V, Kömi J, Porter D (2019) On the role of grain size and carbon content on the sensitization and desensitization behavior of 301 austenitic stainless steel. *Metals.* <https://doi.org/10.3390/met9111193>
- Kavner A, Devine TM (1997) Effect of grain boundary orientation on the sensitization of austenitic stainless steel. *J. Mater. Sci.* 32:1555–1562
- Pradhan SK, Prithiv TS, Mandal S (2017) Through-thickness microstructural evolution during grain boundary engineering type thermomechanical processing and its implication on sensitization behavior in austenitic stainless steel. *Mater. Charact.* 134:134–142
- Kaithwas CK, Bhuyan P, Pradhan SK, Mandal S (2018) Microstructure evolution during low-strain thermo-mechanical processing and its repercussion on intergranular corrosion in alloy 600H. *Mater. Charact.* 145:582–593. <https://doi.org/10.1016/j.matchar.2018.09.019>
- Fujii T, Tohgo K, Mori Y, Shimamura Y (2018) Crystallography of intergranular corrosion in sensitized austenitic stainless steel. *Mater. Charact.* 144:219–226
- Almanza E, Murr LE (2000) A comparison of sensitization kinetics in 304 and 316 stainless steels. *J. Mater. Sci.* 35:3181–3188
- Jinlong L, Hongyun L (2014) Temperature dependence of sensitization on tensile pre-strained AISI 304 stainless steels. *J. Alloys Compd.* 588:509–513. <https://doi.org/10.1016/j.jallcom.2013.11.048>
- Srinivasan N, Kain V, Birbilis N, Kumar BS, Gandhi MN, Sivaprasad PV, Chai G, Lodh A, Ahmedabadi PM, Samajdar I (2016) Plastic deformation and corrosion in austenitic stainless steel: a novel approach through microtexture and infrared spectroscopy. *Corros. Sci.* 111:404–413
- Wasnik DN, Kain V, Samajdar I, Verlinden B, De PK (2002) Resistance to sensitization and intergranular corrosion through extreme randomization of grain boundaries. *Acta. Mater.* 50:4587–4601

27. Shimada M, Kokawa H, Wang ZJ, Sato YS, Karibe I (2002) Optimization of grain boundary character distribution for intergranular corrosion resistant 304 stainless steel by twin-induced grain boundary engineering. *Acta Mater.* 50:2331–2341
28. Srinivasan N, Kumaran SS, Venkateswarlu D (2018) Effects of in-grain misorientation developments in sensitization of 304 L austenitic stainless steels. *Mater. Res. Express.* 6:016551. <https://doi.org/10.1088/2053-1591/aae802>
29. Lai CL, Tsay LW, Kai W, Chen C (2010) The effects of cold rolling and sensitisation on hydrogen embrittlement of AISI 304L welds. *Corros. Sci.* 52:1187–1193. <https://doi.org/10.1016/j.corsci.2009.11.029>
30. Wang Y, Wu X, Li X, Wu W, Gong J (2019) Combined effects of prior plastic deformation and sensitization on hydrogen embrittlement of 304 austenitic stainless steel. *Int. J. Hydrogen Energy.* 44:7014–7031. <https://doi.org/10.1016/j.ijhydene.2019.01.122>
31. Ghosh S, Kain V, Ray A, Roy H, Sivaprasad S, Tarafder S, Ray KK (2009) Deterioration in fracture toughness of 304LN austenitic stainless steel due to sensitization. *Metall Mater. Trans. A Phys. Metall. Mater. Sci.* 40:2938–2949
32. Li S-X, He Y-N, Yu S-R, Zhang P-Y (2013) Evaluation of the effect of grain size on chromium carbide precipitation and intergranular corrosion of 316L stainless steel. *Corros. Sci.* 66:211–216
33. Taiwade RV, Shukla R, Vashishtha H, Ingle AV, Dayal RK (2013) Effect of grain size on degree of sensitization of chrome-manganese stainless steel. *ISIJ Int.* 53:2206–2212. <https://doi.org/10.2355/isijinternational.53.2206>
34. Pradhan SK, Bhuyan P, Mandal S (2018) Individual and synergistic influences of microstructural features on intergranular corrosion behavior in extra-low carbon type 304L austenitic stainless steel. *Corros. Sci.* 139:319–332. <https://doi.org/10.1016/j.corsci.2018.05.014>
35. Jinlong L, Zhuqing W (2019) Sensitization evaluation of the AISI 2205 duplex stainless steel by the IQ value in EBSD technique. *Eng. Fail. Anal.* 105:65–69. <https://doi.org/10.1016/J.ENGFAILANAL.2019.07.001>
36. Barr CM, Thomas S, Hart JL, Harlow W, Anber E, Taheri ML (2018) Tracking the evolution of intergranular corrosion through twin-related domains in grain boundary networks. *Npj Mater. Degrad.* 2:14. <https://doi.org/10.1038/s41529-018-0032-7>
37. Chen AY, Hu WF, Wang D, Zhu YK, Wang P, Yang JH, Wang XY, Gu JF, Lu J (2017) Improving the intergranular corrosion resistance of austenitic stainless steel by high density twinned structure. *Scr. Mater.* 130:264–268. <https://doi.org/10.1016/j.scriptamat.2016.11.032>
38. Zhang R, Qiu Y, Qi Y, Birbilis N (2018) A closer inspection of a grain boundary immune to intergranular corrosion in a sensitised Al-Mg alloy. *Corros. Sci.* <https://doi.org/10.1016/j.corsci.2018.01.009>
39. Maurotto A, Tsvoulas D, Gu Y, Burke MG (2017) Effects of machining abuse on the surface properties of AISI 316L stainless steel. *Int. J. Press. Vessel. Pip.* 151:35–44
40. Srinivasan N, Sunil Kumar B, Kain V, Birbilis N, Joshi SS, Sivaprasad PV, Chai G, Durgaprasad A, Bhattacharya S, Samajdar I (2018) Defining the post-machined sub-surface in austenitic stainless steels. *Metall. Mater. Trans. A.* 49:2281–2292
41. Lyon KN, Marrow TJ, Lyon SB (2015) Influence of milling on the development of stress corrosion cracks in austenitic stainless steel. *J. Mater. Process. Technol.* 218:32–37
42. Ghosh S, Rana VPS, Kain V, Mittal V, Baveja SK (2011) Role of residual stresses induced by industrial fabrication on stress corrosion cracking susceptibility of austenitic stainless steel. *Mater. Des.* 32:3823–3831
43. Kumar PS, Acharyya SG, Rao SVR, Kapoor K (2017) Distinguishing effect of buffing vs. grinding, milling and turning operations on the chloride induced SCC susceptibility of 304L austenitic stainless steel. *Mater. Sci. Eng. A.* 687:193–199
44. Acharyya SG, Khandelwal A, Kain V, Kumar A, Samajdar I (2012) Surface working of 304L stainless steel: impact on microstructure, electrochemical behavior and SCC resistance. *Mater. Charact.* 72:68–76
45. Wang S, Hu Y, Fang K, Zhang W, Wang X (2017) Effect of surface machining on the corrosion behaviour of 316 austenitic stainless steel in simulated PWR water. *Corros. Sci.* 126:104–120
46. Suresh G, Parida PK, Bandi S, Ningshen S (2019) Effect of carbon content on the low temperature sensitization of 304L SS and its corrosion resistance in simulated ground water. *Mater. Chem. Phys.* 226:184–194. <https://doi.org/10.1016/j.matchemphys.2019.01.019>
47. Kolli S, Javaheri V, Ohligschläger T, Kömi J, Porter D (2020) The importance of steel chemistry and thermal history on the sensitization behavior in austenitic stainless steels: experimental and modeling assessment. *Mater. Today Commun.* 24:101088. <https://doi.org/10.1016/j.mtcomm.2020.101088>
48. Pardo A, Merino MC, Carboneras M, Viejo F, Arrabal R, Munoz J (2006) Influence of Cu and Sn content in the corrosion of AISI 304 and 316 stainless steels in H₂SO₄. *Corros. Sci.* 48:1075–1092
49. Farahat AIZ, El-Bitar TA (2010) Effect of Nb, Ti and cold deformation on microstructure and mechanical properties of austenitic stainless steels. *Mat. Sci. Eng. A.* 527:3662–3669
50. Advani AH, Atteridge DG, Murr LE (1991) Solution annealing effects on sensitization of 316 stainless steels. *Scripta Metallurgica Mater.* 25:2221–2226
51. Thorvaldsson T, Dunlop G (1983) Grain boundary Cr-depleted zones in Ti and Nb stabilized austenitic stainless steels. *J. Mater. Sci.* 18:793–803
52. Kim JK, Kim YH, Lee BH, Kim KY (2011) New findings on intergranular corrosion mechanism of stabilized stainless steels. *Electrochim. Acta.* 56:1701–1710
53. Zhang B, Ma X (2019) A review—pitting corrosion initiation investigated by TEM. *J. Mater. Sci. Technol.* 35:1455–1465
54. Verlinden B, Driver J, Samajdar I, Doherty RD (2007) *Thermo Mechanical Processing of Metallic Materials*, 1st edn. Pergamon Materials Series, Great Briton
55. Watanabe Y, Kain V, Tonozuka T, Shoji T, Kondo T, Masuyama F (2000) Effect of Ce addition on the sensitization properties of stainless steels. *Scripta Mater.* 42:307–312
56. Jeon S, Haeng D, Kim H, Park Y (2015) Effect of Ce addition on the precipitation of deleterious phases and the associated intergranular corrosion resistance of 27Cr–7Ni hyper duplex stainless steels. *Corros. Sci.* 90:313–322
57. Watanabe T (1984) Approach to grain boundary design for strong and ductile polycrystals. *Res. Mech.* 11:47–84
58. Watanabe T (2011) Grain boundary engineering: historical perspective and future prospects. *J. Mater. Sci.* 46:4095–4115
59. Jones R, Randle V (2010) Sensitisation behaviour of grain boundary engineered austenitic stainless steel. *Mat. Sci. Eng. A.* 527:4275–4280
60. Owen G, Randle V (2006) On the role of iterative processing in grain boundary engineering. *Scripta Mater.* 55:959–962
61. Engelberg DL, Newman RC, Marrow TJ (2008) Effect of thermomechanical process history on grain boundary control in an austenitic stainless steel. *Scripta Mater.* 59:554–557
62. Engelberg DL, Humphreys FJ, Marrow TJ (2008) The influence of low-strain thermo-mechanical processing on grain boundary network characteristics in type 304 austenitic stainless steel. *J. Microsc.* 230:435–444
63. Michiuchi M, Kokawa H, Wang ZJ, Sato YS, Sakai K (2006) Twin-induced grain boundary engineering for 316 austenitic stainless steel. *Acta Mater.* 54:5179–5184

64. Johnson OK, Schuh CA (2013) The uncorrelated triple junction distribution function: towards grain boundary network design. *Acta Mater.* 61:2863–2873. <https://doi.org/10.1016/j.actamat.2013.01.025>
65. Tsurekawa S, Nakamichi S, Watanabe T (2006) Correlation of grain boundary connectivity with grain boundary character distribution in austenitic stainless steel. *Acta Mater.* 54:3617–3626. <https://doi.org/10.1016/j.actamat.2006.03.048>
66. Rahimi S, Engelberg DL, Marrow TJ (2010) Characterisation of grain boundary cluster compactness in austenitic stainless steel. *Mater. Sci. Technol.* 26:670–675
67. Raveendra S, Kanjarala AK, Paranjape H, Mishra SK, Mishra S, Delannay L, Samajdar I, Vanhoutte P (2011) Strain mode dependence of deformation texture developments: microstructural origin. *Metall. Mater. Trans. A.* 42A:2113–2124
68. Srinivasan N, Kain V, Samajdar I, Krishna KVM, Sivaprasad PV (2017) Plane strain compression testing of Sanicro 28 by channel-die compression test: a direct microstructural observation. *Mater. Today Proc.* 4:9888–9892
69. Hong Y, Zhou C, Zheng Y, Zhang L, Zheng J, Chen X, An B (2018) Formation of strain-induced martensite in selective laser melting austenitic stainless steel. *Mater Sci Eng A.* <https://doi.org/10.1016/j.msea.2018.10.121>
70. Conde A, García I, De Damborenea JJ (2001) Pitting corrosion of 304 stainless steel after laser surface melting in argon and nitrogen atmospheres. *Corros. Sci.* 43:817–828. [https://doi.org/10.1016/S0010-938X\(00\)00114-1](https://doi.org/10.1016/S0010-938X(00)00114-1)
71. Kwok CT, Man HC, Cheng FT (1998) Cavitation erosion and pitting corrosion of laser surface melted stainless steels. *Surf. Coat. Technol.* 99:295–304
72. Mudali UK, Dayal RK, Goswami GL (1995) Desensitisation of austenitic stainless steels using laser surface melting. *Surf. Eng.* 11:331–336. <https://doi.org/10.1179/sur.1995.11.4.331>
73. Parvathavarthini N, Subbarao RV, Kumar S, Dayal RK, Khatak HS (2001) Elimination of intergranular corrosion susceptibility of cold-worked and sensitized AISI 316 SS by laser surface melting. *J. Mater. Eng. Perform.* 10:5–13. <https://doi.org/10.1361/105994901770345277>
74. Mudali UK, Pujar MG, Dayal RK (1998) Effects of laser surface melting on the pitting resistance of sensitized nitrogen-bearing type 316L stainless steel. *J. Mater. Eng. Perform.* 7:214–220. <https://doi.org/10.1361/105994998770347945>
75. Stewart J, Williams DEE (1992) The initiation of pitting corrosion on austenitic stainless steel: on the role and importance of sulphide inclusions. *Corros. Sci.* 33:457–474
76. Hong Y, Zhou C, Zheng Y, Zhang L, Zheng J, Chen X, An B (2019) Formation of strain-induced martensite in selective laser melting austenitic stainless steel. *Mater. Sci. Eng. A.* 740–741:420–426. <https://doi.org/10.1016/j.msea.2018.10.121>
77. De Assis KS, Rocha AC, Margarit-Mattos ICP, Serra FAS, Mattos OR (2013) Practical aspects on the use of on-site double loop electrochemical potentiodynamic reactivation technique (DL-EPR) for duplex stainless steel. *Corros. Sci.* 74:250–255. <https://doi.org/10.1016/j.corsci.2013.04.050>
78. Bose A, De PK (1987) An EPR study on the influence of prior cold work on the degree of sensitization of AISI 304 stainless steel. *Corrosion* 43:624–631
79. De Tiedra P, Martín Ó, López M, San-Juan M (2011) Use of EPR test to study the degree of sensitization in resistance spot welding joints of AISI 304 austenitic stainless steel. *Corros. Sci.* 53:1563–1570
80. Momeni M, Moayed MH, Davoodi A (2010) Tuning DOS measuring parameters based on double-loop EPR in H₂SO₄ containing KSCN by Taguchi method. *Corros. Sci.* 52:2653–2660. <https://doi.org/10.1016/j.corsci.2010.04.015>
81. Kauss N, Heyn A, Halle T, Rosemann P (2019) Detection of sensitisation on aged lean duplex stainless steel with different electrochemical methods. *Electrochim. Acta.* 317:17–24. <https://doi.org/10.1016/j.electacta.2019.05.081>
82. Pujar MG, Parvathavarthini N, Dayal RK, Thirunavukkarasu S (2009) Assessment of intergranular corrosion (IGC) in 316 (N) stainless steel using electrochemical noise (EN) technique. *Corros. Sci.* 51(8):1707–1713
83. Kikuchi H, Sumimoto T, Kamada Y, Kobayashi S (2013) Magnetic NDE for sensitization of Inconel 600 alloy. *J. Magn.* 18:348–351. <https://doi.org/10.4283/JMAG.2013.18.3.348>
84. Xu J, Wu X, Han EH (2013) Acoustic emission response of sensitized 304 stainless steel during intergranular corrosion and stress corrosion cracking. *Corros. Sci.* 73:262–273. <https://doi.org/10.1016/j.corsci.2013.04.014>
85. Ortiz N, Curiel FF, López VH, Ruiz A (2013) Evaluation of the intergranular corrosion susceptibility of UNS S31803 duplex stainless steel with thermoelectric power measurements. *Corros. Sci.* 69:236–244
86. Takaya S, Suzuki T, Matsumoto Y, Demachi K, Uesaka M (2004) Estimation of stress corrosion cracking sensitivity of type 304 stainless steel by magnetic force microscope. *J. Nucl. Mater.* 327:19–26. <https://doi.org/10.1016/j.jnucmat.2004.01.016>
87. Yanliang H, Kinsella B, Becker T (2008) Sensitisation identification of stainless steel to intergranular stress corrosion cracking by atomic force microscopy. *Mater. Lett.* 62:1863–1866. <https://doi.org/10.1016/j.matlet.2007.10.040>
88. Čihal V (1980) A potentiokinetic reactivation method for predicting the I.C.C. and I.G.S.C.C. sensitivity of stainless steels and alloys. *Corros. Sci.* 20:737–744. [https://doi.org/10.1016/0010-938x\(80\)90054-2](https://doi.org/10.1016/0010-938x(80)90054-2)
89. Cihal V, Stefec R, Shoji T, Watanabe T, Kain V (2004) Electrochemical potentiodynamic reactivation: development and applications of the EPR test. *Key. Eng. Mat.* 261–263:855–864
90. Majidi AP, Streicher MA (1984) The double loop reactivation method for detecting sensitization in AISI 304 stainless steels. *Corrosion* 40:584–593
91. Cihal V, Stefec R (2001) On the development of the electrochemical potentiokinetic method. *Electrochim. Acta.* 46:3867–3877. [https://doi.org/10.1016/S0013-4686\(01\)00674-0](https://doi.org/10.1016/S0013-4686(01)00674-0)
92. Doerr C, Kim JY, Singh P, Wall JJ, Jacobs LJ (2017) Evaluation of sensitization in stainless steel 304 and 304L using nonlinear Rayleigh waves. *NDT E Int.* 88:17–23
93. Jothilakshmi N, Nanekar PP, Kain V (2013) Assessment of intergranular corrosion attack in austenitic stainless steel using ultrasonic measurements. *Corrosion* 9312:388–395
94. Remillieux MC, Kaoumi D, Ohara Y, StuberGeesey MA, Xi L, Schoell R, Bryan CR, Enos DG, Summa DA, Ulrich TJ, Anderson BE, Shayer Z (2020) Detecting and imaging stress corrosion cracking in stainless steel, with application to inspecting storage canisters for spent nuclear fuel. *NDT E Int.* <https://doi.org/10.1016/j.ndteint.2019.102180>
95. Doerr C, Lakocy A, Kim JY, Singh PM, Wall JJ, Qu J, Jacobs LJ (2017) Evaluation of the heat-affected zone (HAZ) of a weld joint using nonlinear Rayleigh waves. *Mater. Lett.* 190:221–224. <https://doi.org/10.1016/j.matlet.2017.01.021>
96. Shaikh H, Sivaibharasi N, Sasi B, Anita T, Amirthalingam R, Rao BPC, Jayakumar T, Khatak HS, Raj B (2006) Use of eddy current testing method in detection and evaluation of sensitization and intergranular corrosion in austenitic stainless steels. *Corros. Sci.* 48:1462–1482. <https://doi.org/10.1016/j.corsci.2005.05.017>
97. Kelidari Y, Kashefi M, Mirjalili M, Seyedi M, Krause TW (2020) Eddy current technique as a nondestructive method for evaluating the degree of sensitization of 304 stainless steel. *Corros. Sci.* <https://doi.org/10.1016/j.corsci.2020.108742>

98. Tucker WC, Lockhart P, Guzas E (2019) Evaluating sensitized chromium steel alloys with induction infrared thermography. *J Nondestruct Eval*. <https://doi.org/10.1007/s10921-019-0581-x>
99. Roberts M, Wang K, Guzas E, Lockhart P, Tucker W (2021) Induction infrared thermography for non-destructive evaluation of alloy sensitization. *J. Nondestruct. Eval* 10(1063/1):5099848
100. Fregonese M, Idrissi H, Mazille H, Renaud L, Cetre Y (2001) Initiation and propagation steps in pitting corrosion of austenitic stainless steels: Monitoring by acoustic emission. *Corros. Sci.* 43:627–641. [https://doi.org/10.1016/S0010-938X\(00\)00099-8](https://doi.org/10.1016/S0010-938X(00)00099-8)
101. Mazille H, Rothea R, Tronel C (1995) An acoustic emission technique for monitoring pitting corrosion of austenitic stainless steels. *Corros. Sci.* 37:1365–1375. [https://doi.org/10.1016/0010-938X\(95\)00036-J](https://doi.org/10.1016/0010-938X(95)00036-J)
102. Mukhopadhyay CK, Jayakumar T, Haneef TK, Suresh Kumar S, Rao BPC, Goyal S, Gupta SK, Bhasin V, Vishnuvardhan S, Raghava G, Gandhi P (2014) Use of acoustic emission and ultrasonic techniques for monitoring crack initiation/growth during ratcheting studies on 304LN stainless steel straight pipe. *Int. J. Press. Vessel. Pip.* 116:27–36. <https://doi.org/10.1016/j.ijpvp.2014.01.005>
103. Shaikh H, Amirthalingam R, Anita T, Sivaibharasi N, Jaykumar T, Manohar P, Khatak HS (2007) Evaluation of stress corrosion cracking phenomenon in an AISI type 316LN stainless steel using acoustic emission technique. *Corros. Sci.* 49:740–765. <https://doi.org/10.1016/j.corsci.2006.06.007>
104. Mudali UK, Rao CB, Raj B (2006) Intergranular corrosion damage evaluation through laser scattering technique. *Corros. Sci.* 48:783–796. <https://doi.org/10.1016/j.corsci.2005.02.027>
105. Jingpin J, Junjun S, Guanghai L, Bin W, Cunfu H (2015) NDT & E international evaluation of the intergranular corrosion in austenitic stainless steel using collinear wave mixing method. *NDT E Int.* 69:1–8. <https://doi.org/10.1016/j.ndteint.2014.09.001>
106. Knight SP, Salagaras M, Trueman AR (2011) The study of intergranular corrosion in aircraft aluminium alloys using X-ray tomography. *Corros. Sci.* 53:727–734. <https://doi.org/10.1016/j.corsci.2010.11.005>
107. Ruiz A, Ortiz N, Medina A, Kim JY, Jacobs LJ (2013) Application of ultrasonic methods for early detection of thermal damage in 2205 duplex stainless steel. *NDT E Int.* 54:19–26. <https://doi.org/10.1016/j.ndteint.2012.11.009>
108. Li F, Slusarski K, Xiang D, Qin Y, Pond RB (2010) Measurements of degree of sensitization (DoS) in aluminum alloys using EMAT ultrasound. *Ultrasonics* 51:561–570. <https://doi.org/10.1016/j.ultras.2010.12.009>
109. Stella J, Cerezo J, Rodríguez E (2009) Characterization of the sensitization degree in the AISI 304 stainless steel using spectral analysis and conventional ultrasonic techniques. *NDT E Int.* 42:267–274. <https://doi.org/10.1016/j.ndteint.2008.11.005>
110. Ghanei S, Kashefi M, Mazinani M (2013) Eddy current nondestructive evaluation of dual phase steel. *Mater. Des.* 50:491–496. <https://doi.org/10.1016/j.matdes.2013.03.040>

Publisher's Note Springer Nature remains neutral with regard to jurisdictional claims in published maps and institutional affiliations.